J. Appl. Sci. Innov. Technol. 2 (2), 58-67 (2023) ISSN (Online): 2583-505X

PMSST

Journal of Applied Science, Innovation & Technology (JASIT)

Journal homepage: https://prakritimitrango.com/documents-reports-and-publications/journal/

Research article

Development of Ruthenium metal functionalized gold nanoparticles

Imon Kalyan[1*], Kisor Kumar Sahu[2], Ashish Kumar Nayak[3*]

[1]*School of Nano Science and Technology, IIT Kharagpur, Kharagpur - 721302, West Bengal, India*

[2]*School of Minerals, Metallurgical & Materials Engineering, IIT Bhubaneswar, Bhubaneswar - 752050, Odisha, India*

[3]*Department of Civil Engineering, Prasad V. Potluri Siddhartha Institute of Technology, Vijayawada - 520007, Andhra Pradesh, India*

OPEN ACCESS

ARTICLE INFOR

Article history:

Received: 02 June 2023

Revised: 03 July 2023

Accepted: 04 July 2023

Published online: 04 November, 2023

***Keywords*:**

Gold nanoparticles

Ruthenium

Ruthenium complex

Tetrazine

Functionalization

Surface Plasmon

ABSTRACT

Ruthenium (Ru) and its complex have immense importance in coordination chemistry because of their active applications in bioinorganic chemistry, organometallic chemistry, catalysis, etc. Here, this study will discuss the synthesis of surface-functionalized gold nanoparticles (AuNPs) attached to Ru metal using tetrazine as the bridging ligand. AuNPs have been prepared by slightly modifying the 'Brust' two-phase synthesis method. The Ru complexes have been prepared by the reaction of 6-(3,5-dimethyl-1H-pyrazol-1-yl)-1,2,4,5-tetrazin-3-amine (amtz) with dimeric precursor complex [(*p*-cym)RuCl(μ-Cl)$_2$ (*p*-cym = 1-isopropyl-4methylbenzene)] in methanol. The attachment of the complex on the AuNPs surface has been confirmed by UV-Visible (UV-Vis) spectroscopy. The surface plasmon band that appeared at 523 nm indicates the stability of AuNPs functionalized with Ru complex in the solution.

1. Introduction

Nobel metal nanoparticles-based research has gained significant attention in recent years because of their manifold application in catalysis (Rawat and Singh, 2022a, 2022b), bio-medical, organometallic chemistry, biochemistry, and electronics (Elmes et al., 2011; Gupta et al., 2015; Venkatesan et al., 2013). On the other hand, the development of decorated transition metal complexes with suitable ligand frameworks has also gained momentum because of their utilization in designing models for biological systems (Martínez-Calvo et al., 2016), catalysts for various organic transformations (Comby and Gunnlaugsson, 2011; Valente et al., 2021), and its bioinorganic applications (Ando et al., 2000). These metal-ligand frameworks show interesting structural, redox, catalytic, optical, and electrochemical properties (Betanzos-Lara et al., 2012; Kumar et al., 2018; Schmid, 1992; Segala and Pereira, 2012). Nanoparticles (NPs) have different properties than their bulk counterpart because of the enlarged surface-to-volume ratio, which could be further enhanced by modifying their surface with a suitable metal complex (MC). This type of functionalized metal nano-composite generally has unique synergistic properties along with the individual properties of nanoparticles and metal-complex (Martínez-Calvo et al., 2016). Such surface modification of NPs with MC could be beneficial since such a system can be utilized for the targeted application where combined properties of metal NPs and MC are needed. In addition, such a system allows the confinement of multiple metal centers in a small dimension, leading to functional cooperativity and redox tunability via synergistic interaction between metal ions and NPs (Estalayo-Adrián et al., 2020). Hence, these may exhibit unusual properties with better reactivity and stability than individual subunits. Out of various metal nanoparticles, gold nanoparticles (AuNPs) become attractive due to their size-dependent unique catalytic, electrocatalytic, electronic, and optoelectronic properties (Li et al., 2004; Rycenga et al., 2009; Sebastián et al., 2012). Other

***Corresponding Author:**

E-mail address: imu.kalyan@gmail.com; coco.ashish@gmail.com (A.K. Nayak)

than that AuNPs show less cytotoxicity, biocompatibility and have well-established synthesis procedures in aqueous (Kalyan et al., 2021, 2019) and non-aqueous mediums (Cobley et al., 2008). Also, prepared AuNPs surface could be modified easily and generally have good long-term stability (Dumur et al., 2011; Karthäuser et al., 2020; Khavani et al., 2021; Lewis and Pikramenou, 2014; Martínez-Calvo et al., 2016; Miomandre et al., 2013; Patra et al., 2018; Vilvamani et al., 2016). Another speciality of AuNPs is that both naked and surface-modified NPs show prominent size-dependent plasmonic bands (Patra et al., 2018; Patra and Yang, 2009), which could be easily visualized by UV-vis spectroscopy (Eustis et al., 2006; Park et al., 2007). At the same time among the transition metals Ruthenium (Ru) and its complexes are very popular because of their interesting photo-physical properties and variable oxidation states (Sahoo and Patra, 2020, 2018). Thus Ru complexes have been widely used for the development of catalysts (Dehury et al., 2020; Mishra and Patra, 2023; Patra and Mishra, 2022; Sahoo and Patra, 2018) for various organic transformations and potential anticancer and antibacterial agents (Ando et al., 2000; Carmona et al., 2012; Estalayo-Adrián et al., 2020; Martín Morales et al., 2020; Martínez-Calvo et al., 2016; Meijer et al., 2020; Nasrollahzadeh et al., 2021; Nung Tsai et al., 2015; Rahul and Shekhar, 2021; Szewczyk et al., 2022). Ruthenium metal complexes have been widely tested as anticancer agents (Tripathy et al., 2014), and they are proven to be excellent in case of therapeutic effect on various cancer cell lines (Szewczyk et al., 2022; Valente et al., 2021).

Considering the advantages and exciting features of both AuNPs and ruthenium complexes, the present work will aim to functionalize AuNPs with Ru MC with suitable bridging ligands for the development of hybrid materials of metal complex-tethered-AuNPs. (Cymene)ruthenium chloride {(*p*-cym)RuCl} fragment has been selected to prepare metal complexes considering its unique photochemical properties, persuasive biological activity, and widespread applications as catalysts for various organic transformations (Tripathy et al., 2014).

In order to achieve metal complex-tethered-AuNPs suitable ligand framework is required to act as a bridge between AuNP and the metal unit. Tetrazine and its derivatives are promising candidates in this regard owing to their excellent coordination chemistry, non-innocent behavior, and ability to hold both metal center and nanoparticles (Kaim, 2002). Moreover, the low-lying π^* orbital localized at the four nitrogen atoms exhibits intense low-energy charge transfer absorptions, the electrical conductivity of coordination polymers, and exceptional stability of paramagnetic radical or mixed-valent intermediates.

So, in this work, at first, ligand 6-(3,5-dimethyl-1H-pyrazol-1-yl)-1,2,4,5-tetrazin-3-amine (amtz) was prepared, which indicated as Ligand 1 (Scheme 1). In the next step, the precursor complex [(*p*-cym)RuCl(μ-Cl)$_2$ (*p*-cym = 1-isopropyl-4methylbenzene)] was synthesized, which is designated as Precursor Complex 2 (Scheme 1). After that, with the help of Precursor Complex 2 and Lgand 1, amine group (-NH_2) pendent Ru-MC (Rutheniummetal complex) was prepared, which represented as Ruthenium(II) Complex 3 (Scheme 1). Finally, tetraoctylammoniumbromide (TOAB) stabilized gold nanoparticles (AuNPs) were prepared in the toluene phase and then functionalized these AuNPs with Ruthenium(II) Complex 3.

2. Experimental Section

2.1. Materials and Instrumentation

All chemicals were used standard grade, obtained from Sigma Aldrich and Spectrochem. Ultrapure triple distilled water (Millipore-Q Water system) was used to prepare all aqueous solutions. Centrifugation was performed by the velocity 18R, refrigerated centrifuge. UV-Vis spectra of nanoparticle solutions were acquired by Perkin Elmar Lambda 35 UV-Vis spectrophotometer.

2.2. Preparation of Ligand 1

The ligand 6-(3,5-dimethyl-1H-pyrazol-1-yl)-1,2,4,5-tetrazin-3-amine (amtz) (Ligand 1) was prepared according to the reported procedure (Scheme 2) (Bennett et al., 1982). 3,6-bis(3,5-dimethylpyrazol-1-yl)-1,2,4,5-tetrazin (bpytz) (400 mg, 1.48 mmol) was taken in 30 cm^3 toluene and stirred vigorously for 1 h at -20 °C. Then, 0.11 mL, 25% ammonia solution was added and further stirred for 10 h at room temperature. During the course of the reaction the color of the solution changed from reddish-pink to orange. After completion, the volume of the solution was reduced to 3 cm^3 using a rotary evaporator. The bright orange colored precipitate was separated out from the solution. The precipitate was filtered, washed thoroughly with toluene, and dried in air to get pure Ligand 1.

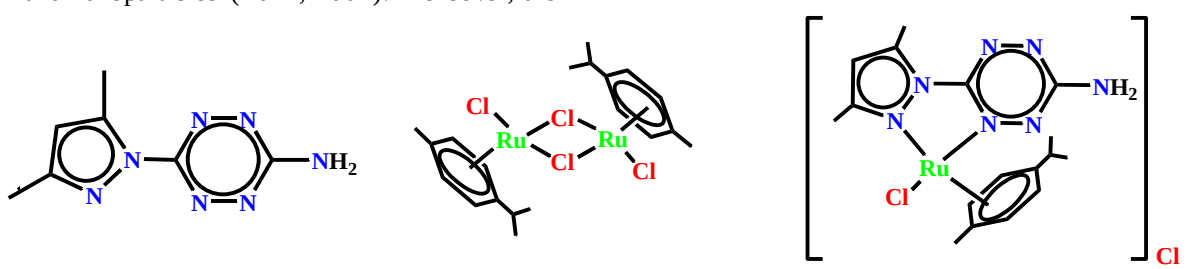

Ligand 1 **Precursor Complex 2** **Ruthenium (II) Complex 3**

a) **b)** **c)**

Scheme 1. Chemical structures of a) Ligand 1, b) Precursor Complex 2, and c) Ruthenium(II) Complex 3

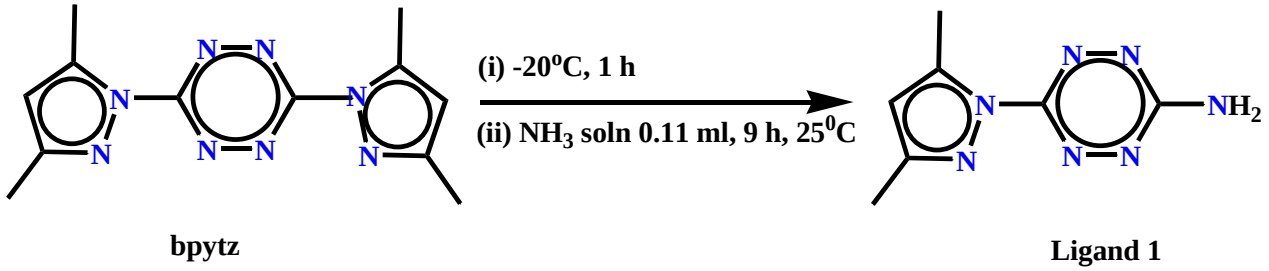

Scheme 2. Preparation of Ligand 1

2.3. Preparation of Precursor Complex 2

The precursor complex [(*p*-cym)RuCl(μ-Cl)$_2$ (*p*-cym = 1-isopropyl-4methylbenzene)] (Precursor Complex 2) was synthesized by following the reported procedure (Scheme 3) (Nayak et al., 2005).

An amount of 1.0 g of $RuCl_3$, $3H_2O$ (Ruthenium (III) chloride trihydrate) was dissolved in 50 cm^3 of ethanol and 5 cm^3 of α-phellandrene was added into it. The mixture was refluxed for 8 h with continuous stirring. The volume of the brown colored solution obtained was reduced under vacuum and kept at 4 °C overnight and washed with cold ethanol and dried in an air.

2.4. Preparation of Ruthenium(II) Complex 3

About 65 mg of 0.1 mmol Precursor Complex 2 and 40 mg of 0.2 mmol Ligand 1 were taken in 25 cm^3 of methanol and heated to reflux for 12 h (Scheme 4). The initial orange red color of the reaction mixture turned into dark brown during the course of the reaction. After completion, the reaction mixture was dried completely using a rotary evaporator. Then the precipitate was purified using a silica gel column with dichloromethane: methanol (8:1) as eluent; yield: 60 mg (57%) and molar conductivity [$\Lambda_M/(\Omega^{-1}$ cm^2 dm^3 mol^{-1})] in acetonitrile was found to be 110. The positive ion electrospray mass spectrum of Ruthenium(II) Complex 3 in methanol exhibited the signal centered at m/z value of 461.95 corresponding to{3-Cl}$^+$ (calculated molar mass is 461.97 g/mol). ^{1}H NMR: δ_{ppm}= 8.2 (s, 2H{NH_2}), 6.2 (s, 1H{$Ar_{p\text{-}cy}$}), 6.089 (t, 1H{$Ar_{p\text{-}cy}$}), 5.948(d, 1H{$Ar_{p\text{-}cy}$}), 1.8 (m, 1H{$CH(CH_3)_2$}, 2.6 (d, 3H{$CH(CH_3)_2$}), 2.3 (d, 3H{$CH(CH_3)_2$}). λmax/nm (ε/ dm3 mol^{-1} cm^{-1}) in acetonitrile: 499 (2200), 279 (10800).

2.5. Synthesis of Au Nanoparticles (AuNPs)

AuNPs have been prepared with a slight modification of the "Brust" two-phase synthesis (Brust et al., 1994). The process is briefly described as follows: Bright yellow colored aqueous solution of $HAuCl_4{\cdot}3H_2O$ (2.36 μM) was taken 12 mL in a Round Bottom flask followed by 48 mL tetraoctylammoniumbromide (TOAB) (39.3μM), toluene solution (colorless) and stirred vigorously for 15 minutes until all the gold ions transferred into the toluene phase. The completion of the transfer of Gold ions into the toluene phase can be recognized by the change of color of the toluene phase into bright yellow from colorless and the water phase become colorless from bright yellow. Reducing agent $NaBH_4$ (0.4 mol L^{-1}) of 12 mL aqueous solution was then added to the flask with continuous stirring, and the solution turned into a wine red color, indicating the formation of Nanoparticles. The change of this color is instant. These AuNPs show absorbance at 523 nm in UV-Vis spectroscopy, as shown below (Fig. 4).

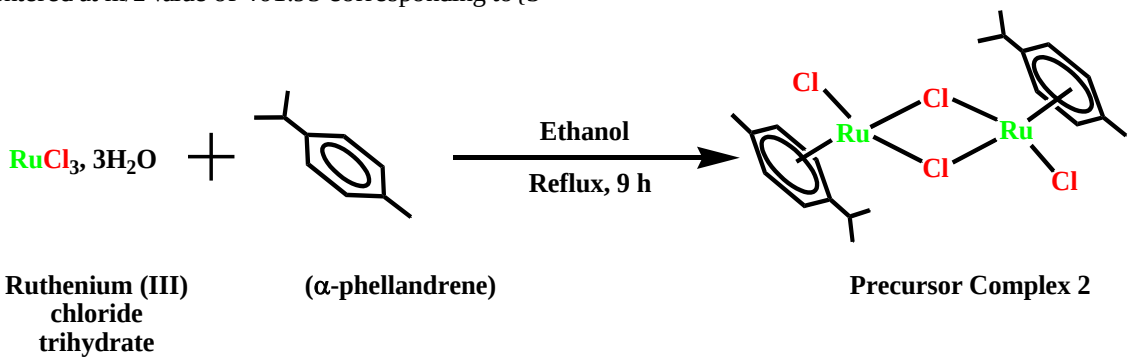

Scheme 3. Preparation of Precursor Complex 2

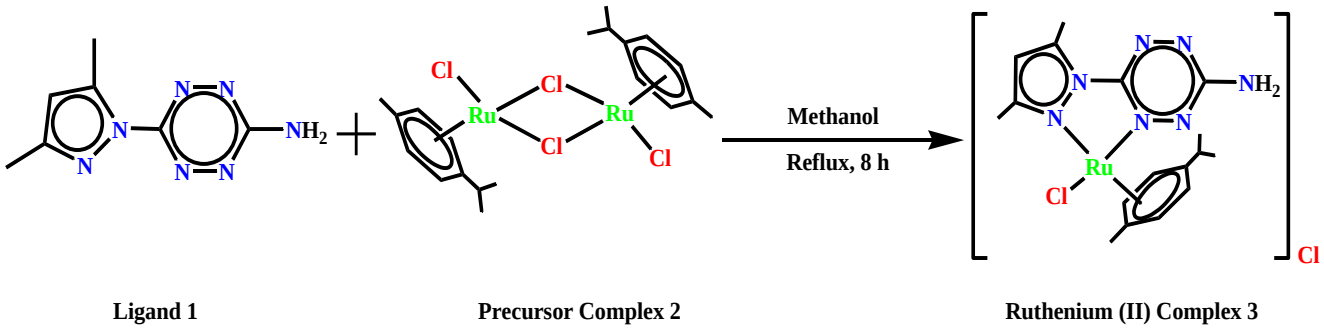

Scheme 4. Preparation of Ruthenium(II) Complex 3

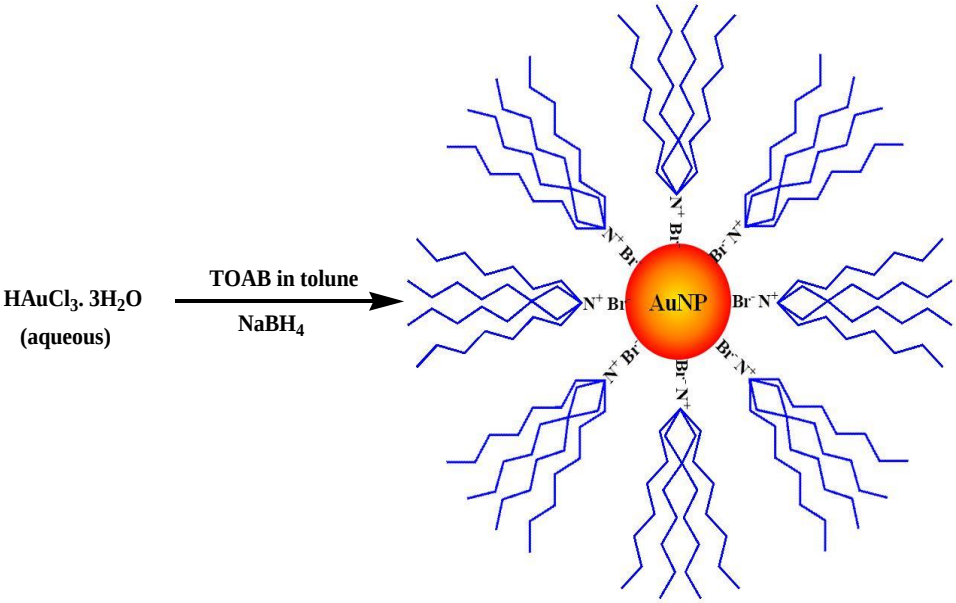

Scheme 5. Preparation of TOAB stabilized AuNPs in toluene

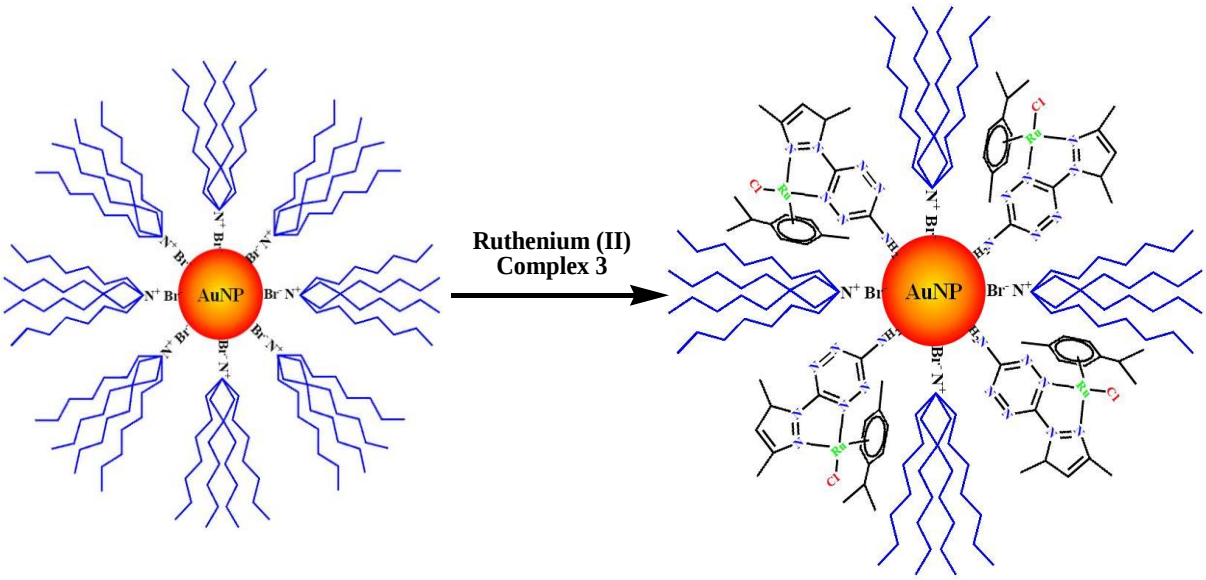

Scheme 6. Preparation of Ruthenium (II) complex 3 modified AuNPs

2.6. Preparation of Ruthenium (II) Complex 3 modified AuNPs

The capability of Ruthenium(II) Complex 3 to effectively coat and stabilize gold NPs in the toluene phase should be due to the ($-NH_2$) group, which has much greater binding interaction than that of weakly bounded TOAB, which was used as phase transfer agent as well as a surface stabilizer. To coat and stabilize, 10 mL (0.0058 mmol) nanoparticle solution was taken in a round-bottom flask, and then 20 mL (0.0029 mmol) aqueous complex solution was added drop-wise (as shown in Scheme 6), resulting in the biphasic system of toluene and water. The biphasic system was then vigorously stirred for one hour, leading to a discoloration of the aqueous phase while the originally wine red toluene phase turned deep red. Now this system consists of AuNPs which suface is covered with Ruthenium (II) Complex 3 as well partially with small amount of TOAB also. After addition of complex there might be excess complex in the solution other than the complex attached to the surface of the AuNP. The excess complex was removed by centrifugation. Centrifugation has been done in 14000 rpm at 0^0 C for two and a half hours. Then we have decanted the excess complex solution and then re-dispersed the precipitate (Ruthenium (II) Complex 3 attached AuNPs) in toluene, and then UV-Vis spectroscopy was performed.

3. Results and Discussion

This section focuses on the complete characterization of the Ruthenium (II) complex 3 by means of various characterization techniques like "Mass spectroscopy," "^{1}H NMR spectra", "Cyclic voltammogram," "UV-Vis spectra," etc. The complex 3 attached AuNPs have also been characterized by "UV-Vis spectroscopy."

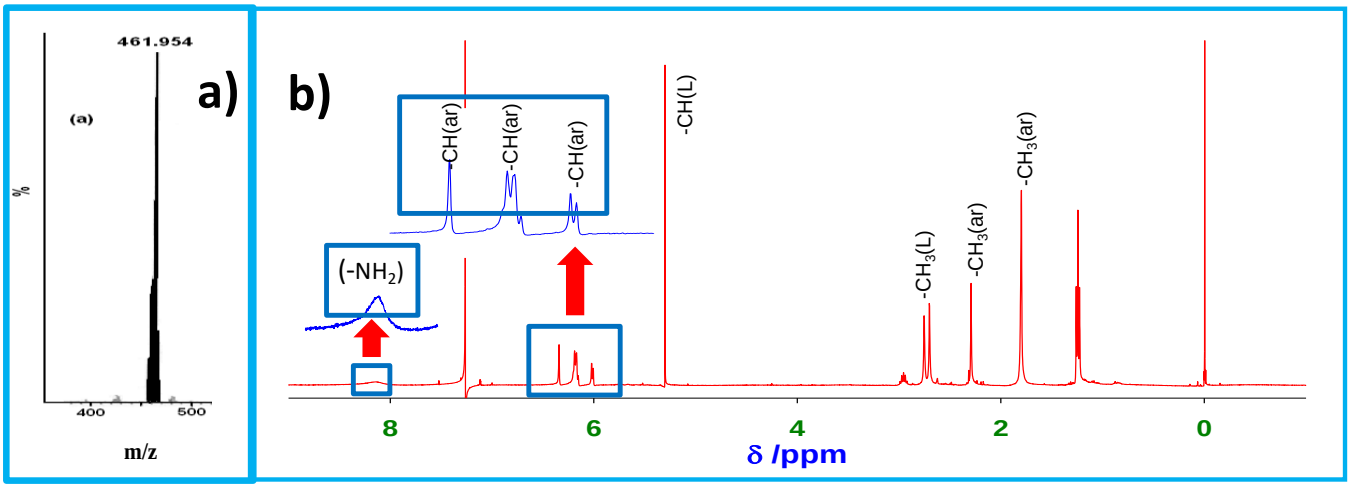

Fig. 1 a) Electrospray Mass Spectra of Ruthenium (II) complex 3 in CH_3OH and, b) NMR spectra of Ruthenium (II) complex 3 in $CDCL_3$.

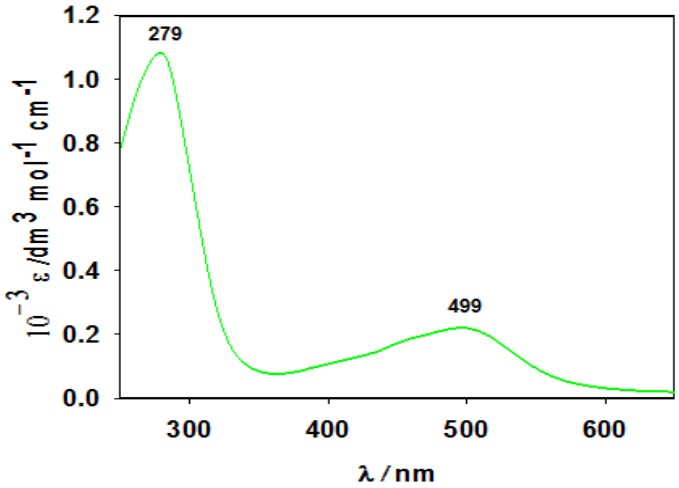

Fig. 2. UV-Vis spectra of Ruthenium (II) complex 3

3.1. Mass spectra

Mass spectrometers use the difference in mass-to-charge ratio (*m*/*z*) of ionized atoms or molecules to separate them. Therefore, mass spectroscopy allows the quantification of atoms or molecules and provides structural information by the identification of distinctive fragmentation patterns. The positive ion ESI (Electrospray ionization) mass spectrum in CH_3OH **(Fig. 1a)** shows molecular ion peaks at 461.95 for [**2**-Cl]$^+$(calculated: 461.97), which supports its identity in solution. This spectra is showing the exact match with the calculated value of 461.97, which supports the formation of the desired Ruthenium (II) complex 3.

3.2. NMR spectra

The formation of the Ruthenium (II) complex 3 has been authenticated by ^{1}H NMR spectra (Fig. 1b)). ^{1}H NMR further spectra of the complex 3 in $CDCl_3$ showed the presence of expected peaks at δ_{ppm}= 8.2 (s, 2H{NH_2}), 6.2 (s, 1H{$Ar_{p\text{-}cy}$}), 6.089 (t, 1H{$Ar_{p\text{-}cy}$}), 5.948(d, 1H{$Ar_{p\text{-}cy}$}), 1.8 (m, 1H{$CH(CH_3)_2$}, 2.6 (d, 3H{$CH(CH_3)_2$}), 2.3 (d, 3H{$CH(CH_3)_2$}).

3.3. UV-Vis Spectra

The chloride Ruthenium (II) complex 3 displays lowest energy MLCT (metal-to-ligand-charge transfer) at 499 nm and intra-ligand transition in the UV region at 279 nm in UV-Vis spectroscopy **(Fig. 2)**.

3.4. Electron transfer Properties

Cyclic voltammetric studies of Ruthenium (II) complex 3 have been performed in acetonitrile solvent using tetraethyl ammonium perchlorate (TEAP) as supporting electrolyte, Ag/AgCl as reference electrode and Pt as working electrode.

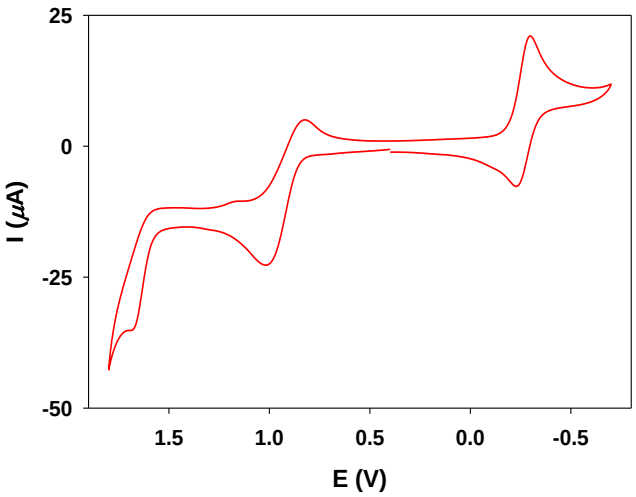

Fig. 3. Cyclic voltammograms of Ruthenium (II) complex 3 in CH_3CN 0.1 mol dm^{-3} Et_4NClO_4 *versus* Ag/AgCl (scan rate 50 mV s^{-1}).

The cyclic voltammograms of the Ruthenium (II) complex 3 **(Fig. 3)** has showed a quasi-reversible peak at 0.9 V corresponding to oxidation of metal centre (Ru^{II}/Ru^{III}). In addition to that an irreversible peak at 1.7 corresponding further oxidation of the metal centre (Ru^{III}/Ru^{IV}) and a reversible peak at -0.28V corresponding to the reduction of tetrazine ligand has also been obtained.

3.5. Spectral Studies of Ruthenium (II) complex 3-AuNPs conjugate

The AuNPs in toluene show absorbance at 523 nm in UV-Vis spectroscopy, as shown below (Fig. 4, Red Curve). This indicates the expected average particle size 5±2 nm. This can be concluded with the basis of the absorbance curve given in the reference (Mayer et al., 2008). The given absorbance graph is the exact match with the study of Mayer et al. (2008). The graph here is also indicative of the precise reproducibility of the system. Complex attached AuNPs showed two different absorbance peaks at 422 nm and 522 nm suggesting that the complex was attaching to the surface of the AuNPs. After addition of complex to the Gold nanoparticles excess complex was removed by centrifugation. Then UV-Vis spectra of the system were analyzed. In Fig. 4 comparison of UV-Vis spectra AuNPs and Ruthenium (II) complex 3 added AuNPs before centrifuge (Green curve) and after centrifuge (Blue curve) are shown. Thus, the Ruthenium (II) complex 3 bearing a ($-NH_2$) group is therefore very efficient in binding with Au-NPs and formed a stable Au-NP complex system in the toluene phase (Scheme 5).

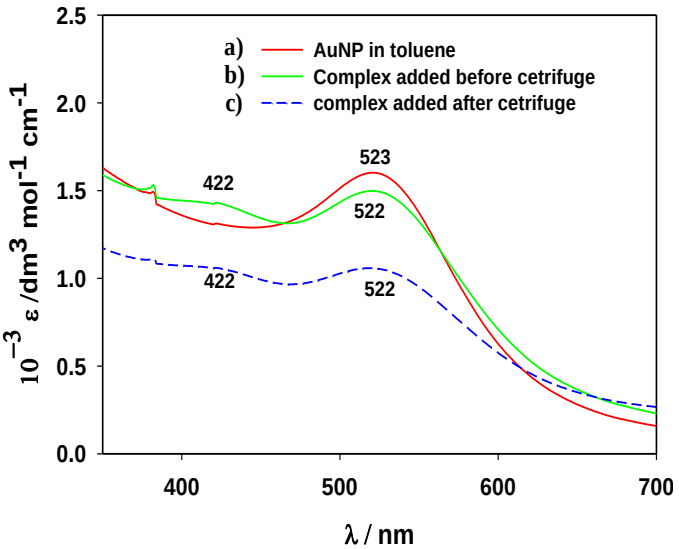

Fig. 4. UV-Vis spectra of a) AuNP in toluene, b) Ruthenium (II) complex 3 added AuNPs before centrifuge, and c) Ruthenium (II) complex 3 added AuNPs after centrifuge.

4. Cost Analysis

Cost analysis is an important aspect of evaluating the real field utility of the prepared material. In this study, the cost estimation is complicated. So, this study only considering the cost of the important materials to calculate this multi stage work. Other expenses like each time cleaning, drying before and after each reaction, etc., were calculated as "Other miscellaneous cost." All the expenses have been calculated in Indian Rupees (INR) with the most recent approximate materials and electricity rates. Table 1 shows the price of important materials. In this study, the cost of the main materials (Ligand 1, Precursor Complex 2, Ruthenium(II) Complex 3, Au Nanoparticles (AuNPs), and Ruthenium(II) Complex 3 modified AuNPs) was calculated. The cost of preparation of Ligand 1 is shown in Table 2. The cost of preparation of Precursor Complex 2 is shown in Table 3. The cost of preparation of Ruthenium(II) Complex 3 is shown in Table 4. The cost of preparation of Au Nanoparticles (AuNPs) is shown in Table 5. Finally, the cost of preparing 1 ml Ruthenium(II) Complex 3 modified AuNPs is calculated.

4.1. Cost Analysis of Preparation of Ligand 1

Here in Table 2, details of expenditure for the preparation of Ligand 1 are shown. Finally 1 g Ligand 1 price is determined.

Ligand 1 yield is 95%. Therefore, almost 0.380 g of product is formed from 0.400 g of raw material. Consequently, the cost of the final product of 0.380 g is 5459.42 INR. The cost of 1 gram of the final product will be almost 14367.00 INR.

4.2. Cost Analysis of Preparation of Precursor Complex 2

A detailed cost analysis of Precursor Complex 2 preparation is shown in Table 3. Finally, 1 g Precursor Complex 2 price is determined.

Precursor Complex 2 yield was 90%. Accordingly, almost 0.9 g of product was formed from 1g of raw material. So, the cost of 0.9 g of the final product will be 8107.20 INR. Now, the 1 g final product cost will be almost 9008.00 INR.

4.3. Cost Analysis of Preparation of Ruthenium (II) Complex 3

Table 4 depicts details of the cost of the preparation of Ruthenium (II) Complex 3. Ultimately 1 g Ruthenium (II) Complex 3 price is calculated.

Ruthenium (II) Complex 3 yield is 57%, and 0.060 g product is formed. So, 0.06 g costs 1371.30 INR. Now 1 g will cost almost 22855.00 INR.

4.4. Cost Analysis of Au Nanoparticles (AuNPs) preparation

The molecular weight of $HAuCl_4 \cdot 3H_2O$ is 393.83, and the molecular weight of TOAB is 546.79.

So a total of 60 mL (12 mL $HAuCl_4 \cdot 3H_2O$ + 48 mL TOAB + 12 mL l $NaBH_4$) AuNPs costs 52.85 INR. That means 1 mL AuNPs will cost 0.88 INR.

4.5. Cost Analysis of Ruthenium (II) Complex 3 modified AuNPs

Ruthenium (II) Complex 3 has a molecular weight of 461.97. So, 20 ml 0.0029 mmol will cost 0.60 INR.

So total 30 ml (10 ml AuNPs + 20 ml Ruthenium(II) Complex 3) Ruthenium(II) Complex 3 modified AuNPs will cost (10× 0.88 + 0.60) = 9.40 INR. So, 1 ml Ruthenium (II) Complex 3 modified AuNPs will cost 0.31 INR.

Therefore, it can be realized from the study that though the starting materials needed to perform these reactions are much costlier, the final complex modified gold nanoparticles are much cheaper to produce and can potentially be used in different reactions. So, it is understandable that final product actually consist of very few gold or ruthenium in it.

Table 1. Price of Important Materials

Serial No.	Name of the materials	Company	Quantity	Price (INR)
1	Toluene	Spectrochem	1 L	700.00
2	3,6-bis(3,5-dimethylpyrazol-1-yl)-1,2,4,5-tetrazin	Sigma	1 g	13200.00
3	Ammonium hydroxide solution	Sigma	5 ml	3910.00
4	Ruthenium(III) chloride trihydrate	Sigma	10 g	76100.00
5	Ethanol	Spectrochem	1 L	600.00
6	Methanol	Spectrochem	1 L	740.00
7	α-phellandrene	Sigma	100 ml	5600.00
8	$HAuCl_4 \cdot 3H_2O$	Sigma	1 g	14367.00
9	Tetraoctylammonium bromide (TOAB)	Sigma	5 g	2200.00

Table 2. Cost of preparation of Ligand 1

Serial No.	Name	Price per unit	Quantity used	Net price (INR)
1	3,6-bis(3,5-dimethylpyrazol-1-yl)-1,2,4,5-tetrazin (bpytz)	13200.00 INR/g	400 mg	5280.00
2	Cooling cost	7.00 INR/kWh	4 kWh (1 h at -20 °C)	28.00
3	Stirring cost	7.00 INR/kWh	0.2 kWh (600 rpm for 1 h)	01.40
4	Ammonium hydroxide solution	782.00 INR/ml	0.11 ml	86.02
5	Stirring cost	7.00 INR/kWh	2 kWh (600 rpm for 10 h)	14.00
6	Other miscellaneous cost (Like Drying, cleaning etc.	NA	NA	50.00
7	Total cost			5459.42

Table 3. Cost of preparation of Precursor Complex 2

Serial No.	Name	Price per unit	Quantity used	Net price (INR)
1	$RuCl_3$, $3H_2O$	7610.00 INR/g	1 g	7610.00
2	α-phellandrene	56.00 INR/ml	5 ml	280.00
3	Ethanol	0.60 INR/ml	100 ml (50 ml for synthesis & 50 ml for washing)	60.00
3	Stirring cost	7.00 INR/kWh	1.6 kWh (600 rpm for 8 h)	11.20
4	Heating cost	7.00 INR/kWh	12 kWh (8 h)	96.00
5	Other miscellaneous cost (Like Drying, cleaning, etc.)	NA	NA	50.00
6	Total cost			8107.20

Table 4. Cost of preparation Ruthenium (II) Complex 3

Serial No.	Name	Price per unit	Quantity used	Net price (INR)
1	Ligand 1	14367.00 INR/g	0.04 g	574.00
2	Precursor Complex 2	9008.00 INR/g	0.065 g	586.00
3	Methanol	0.74 INR/ml	25 ml	18.50
3	Stirring cost	7.00 INR/kWh	2.4 kWh (600 rpm for 12 h)	16.80
4	Heating cost	7.00 INR/kWh	18 kWh (8 h)	126.00
5	Other miscellaneous cost (Like Drying, cleaning etc.	NA	NA	50.00
6	Total cost			1371.30

Table 5. Cost of preparation Au Nanoparticles (AuNPs)

Serial No.	Name	Price per unit	Quantity used	Net price (INR)
1	$HAuCl_4 \cdot 3H_2O$	14367.00 INR/g	0.000116 g	1.70
2	Tetraoctylammoniumbromide (TOAB)	440.00 INR/g	0.001032 g	0.45
3	Stirring cost	7.00 INR/kWh	0.1 kWh (600 rpm for 1/2 h)	0.70
5	Other miscellaneous cost (Like Drying, cleaning etc.	NA	NA	50.00
6	Total cost			52.85

5. Conclusions

Tetraoctylammoniumbromide (TOAB) stabilized gold nanoparticles (AuNPs) in the toluene phase, amtz Ligand 1, and Ruthenium (II) complex 3 are synthesized and characterized using various analytical techniques. The Surface of AuNPs is modified by using Ruthenium (II) complex 3. Attachment of the complex on the nanoparticle surface and stabilization of the system has been observed from the UV-Vis spectra. Further characterization and application of the system are under investigation.

The key findings of the study are given as follows:

1) The AuNPs prepared here in a non-aqueous toluene phase could be beneficial for the application where operating in aqueous phase is not possible.

2) The conjugation of AuNPs with Ruthenium (II) complex 3 happened because of the presence of $-NH_2$ group.

3) The conjugation of AuNPs with Ruthenium (II) complex 3 is very stable and also proves that AuNPs have the preferential binding ability with an amine group ($-NH_2$) like the thiol group (-SH).

4) The above study also proves that the amine-AuNPs interaction is media independent interaction as the system is synthesized in non-aqueous toluene phase.

5) The ultimate cost to produce Ru-MC functionalized with AuNPs material is cheap and could be used in different applications.

Conflict of interest

The author declares no conflict of interest.

Contribution of authors

Dr. Ashish Kumar Nayak (Assistant Professor) helped to prepare the manuscript and plagiarism check. **Dr. Kisor Kumar Sahu (Assistant Professor)** has supervised the experiment. **Dr. Imon Kalyan** conducted all the experiments and prepared the manuscript draft.

Acknowledgments

We want to thank Dr. Srikanta Patra of the "School of Basic Science," IIT Bhubaneswar, for providing the laboratory facility and the initial conceptualizing of the work. We are grateful to the "Minerals, Metallurgical & Materials Engineering" of IIT Bhubaneswar for providing an all-important research facility. We also thank MHRD, Govt. of India, for the necessary funding. We also appreciate the help of Dr. Kisor Kumar Sahu, the "Minerals, Metallurgical & Materials Engineering" of IIT Bhubaneswar, and Dr. Ashish Kumar Nayek in preparing the manuscript.

References

Ando, T., Kamigaito, M., Sawamoto, M., 2000. Catalytic activities of Ruthenium(II) complexes in transition metal-mediated living radical polymerization: Polymerization, model reaction, and cyclic coltammetry. Macromol. 33(16), 5825-5829.

Bennett, M.A., Huang, T., Matheson, T.W., Smith, A.K., Ittel, S., Nickerson, W., 1982. 16.(η6-Hexamethylbenzene) ruthenium complexes. Inorg. Synth. 21, 74–78.

Betanzos-Lara, S., Liu, Z., Habtemariam, A., Pizarro, A.M., Qamar, B., Sadler, P.J., 2012. Organometallic ruthenium and iridium transfer-hydrogenation catalysts using coenzyme NADH as a Cofactor. Angew. Chem. Int. Ed. 124(16), 3963–3966.

Brust, M., Walker, M., Bethell, D., Schiffrin, D.J., Whyman, R., 1994. Synthesis of thiol-derivatised gold nanoparticles in a two-phase liquid-liquid system. J. Chem. Soc., Chem. Commun. (7), 801–802.

Carmona, D., Viguri, F., Pilar Lamata, M., Ferrer, J., Bardají, E., Lahoz, F.J., García-Orduña, P., Oro, L.A., 2012. Ruthenium amino carboxylate complexes as asymmetric hydrogen transfer catalysts. Dalt. Trans. 41(34), 10298–10308.

Cobley, C.M., Campbell, D.J., Xia, Y., 2008. Tailoring the optical and catalytic properties of gold-silver nanoboxes and nanocages by introducing palladium. Adv. Mater. 20(4), 748.

Comby, S., Gunnlaugsson, T., 2011. Luminescent lanthanide-functionalized gold nanoparticles: Exploiting the interaction with bovine serum albumin for potential sensing applications. ACS Nano. 5(9), 7184–7197.

Dehury, N., Mishra, S.R., Laha, P., Patra, S., 2020. Tandem α/β-alkylation and transfer hydrogenation by heterodimetallic ruthenium-iridium complex. Inorganica Chim. Acta. 511, 119796.

Dumur, F., Guerlin, A., Dumas, E., Bertin, D., Gigmes, D., Mayer, C.R., 2011. Controlled spontaneous generation of gold nanoparticles assisted by dual reducing and capping agents. Gold Bull. 44(2), 119–137.

Elmes, R.B.P., Orange, K.N., Cloonan, S.M., Williams, D.C., Gunnlaugsson, T., 2011. Luminescent ruthenium(II) polypyridyl functionalized gold nanoparticles; Their DNA binding abilities and application as cellular imaging agents. J. Am. Chem. Soc. 133(40), 15862–15865.

Estalayo-Adrián, S., McManus, G.J., Dalton, H.L., Savyasachi, A.J., Kelly, J.M., Gunnlaugsson, T., 2020. Functionalisation of gold nanoparticles with ruthenium(II) polypyridyl complexes for their application in cellular imaging. Dalt. Trans. 49(40), 14158–14168.

Eustis, S., El-sayed, M.A., Kasha, M., 2006. Why gold nanoparticles are more precious than pretty gold : Noble metal surface plasmon resonance and its enhancement of the radiative and nonradiative properties of nanocrystals of different shapes. Chem. Soc. Rev. 35(3), 209–217.

Gupta, R.K., Dubey, M., Li, P.Z., Xu, Q., Pandey, D.S., 2015. Size-controlled synthesis of Ag nanoparticles functionalized by heteroleptic dipyrrinato complexes having meso-pyridyl substituents and their catalytic applications. Inorg. Chem. 54(6), 2500–2511.

Kaim, W., 2002. The coordination chemistry of 1,2,4,5-tetrazines. Coord. Chem. Rev. 230(1–2), 127–139.

Kalyan, I., Pal, T., Pal, A., 2021. Immobilization of size variable Au nanoparticles on surfactant-modified silica and their catalytic application toward 4-nitrophenol reduction: A comparative account of catalysis. Surf. Interfaces. 26, 101423.

Kalyan, I., Pal, T., Pal, A., 2019. Time and temperature dependent formation of hollow gold nanoparticles via galvanic replacement reaction of As(0) and its catalytic application. MRS Commun. 9(1), 270–279.

Karthäuser, S., Peter, S., Simon, U., 2020. Integration of individual functionalized gold nanoparticles into nanoelectrode configurations: Recent advances. Eur. J. Inorg. Chem. 2020(40), 3798–3810.

Khavani, M., Mehranfar, A., Izadyar, M., 2021. A theoretical

approach on the ability of functionalized gold nanoparticles for detection of Cd^{2+}. Sci. Rep. 11(1), 23422.

Kumar, P., Li, Z., Wong, S.L., 2018. "Functionalized transition metal dichalcogenide-based nanomaterials for biomedical applications" in Sarmento, B., das Neves, J. "*Biomedical Applications of Functionalized Nanomaterials*", Elsevier.

Lewis, D.J., Pikramenou, Z., 2014. Lanthanide-coated gold nanoparticles for biomedical applications. Coord. Chem. Rev. 273, 213–225.

Li, X.H., Li, Y.C., Tan, Y.W., Yang, C.H., Li, Y.F., 2004. Self-assembly of gold nanoparticles prepared with 3,4-ethylenedioxythiophene as reductant. J. Phys. Chem. B. 108(17), 5192–5199.

Martín Morales, E., Coppel, Y., Lecante, P., Del Rosal, I., Poteau, R., Esvan, J., Sutra, P., Philippot, K., Igau, A., 2020. When organophosphorus ruthenium complexes covalently bind to ruthenium nanoparticles to form nanoscale hybrid materials. Chem. Commun. 56(29), 4059–4062.

Martínez-Calvo, M., Orange, K.N., Elmes, R.B.P., La Cour Poulsen, B., Williams, D.C., Gunnlaugsson, T., 2016. Ru(II)-polypyridyl surface functionalised gold nanoparticles as DNA targeting supramolecular structures and luminescent cellular imaging agents. Nanoscale. 8(1), 563–574.

Mayer, C.R., Dumas, E., Sécheresse, F., 2008. 1,10-Phenanthroline and 1,10-phenanthroline-terminated ruthenium(II) complex as efficient capping agents to stabilize gold nanoparticles: Application for reversible aqueous-organic phase transfer processes. J. Colloid Interface Sci. 328(2), 452–457.

Meijer, M.S., Natile, M.M., Bonnet, S., 2020. 796 nm Activation of a photocleavable ruthenium(II) complex conjugated to an upconverting nanoparticle through two phosphonate groups. Inorg. Chem. 59(20), 14807–14818.

Miomandre, F., Stancheva, S., Audibert, J.F., Brosseau, A., Pansu, R.B., Lepeltier, M., Mayer, C.R., 2013. Gold and silver nanoparticles functionalized by luminescent iridium complexes: Synthesis and photophysical and electrofluorochromic properties. J. Phys. Chem. C. 117(24), 12806–12814.

Mishra, S., Patra, S., 2023. Heterodimetallic iridium-rhenium system: Synthesis, computational and photocatalytic aspects. J. Photochem. Photobiol. A Chem. 436, 114407.

Nasrollahzadeh, M., Soleimani, F., Bidgoli, N.S.S., Nezafat, Z., Orooji, Y., Baran, T., 2021. Recent developments in polymer-supported ruthenium nanoparticles/complexes for oxidation reactions. J. Organomet. Chem. 933, 121658.

Nayak, A., Patra, S., Sarkar, B., Ghumaan, S., Puranik, V.G., Kaim, W., Lahiri, G.K., 2005. Tetrazine derived mononuclear $Ru^{II}(acac)_2(L)$ (1), $[Ru^{II}(bpy)_2(L)](ClO_4)_2$ (2) and $[Ru^{II}(bpy)(L)_2](ClO4)2$ (3) (L = 3-amino-6-(3,5-dimethylpyrazol-1-yl)-1,2,4,5-tetrazine, acac = acetylacetonate, bpy = 2,2′-bipyridine): syntheses, structures, spectra and redox properties. Polyhedron. 24(2), 333–342.

Nung Tsai, C., Mazumder, S., Zhu Zhang, X., Bernhard Schlegel, H., Jang Chen, Y., Endicott, J.F., 2015. Metal-to-ligand charge-transfer emissions of ruthenium(II) pentaammine complexes with monodentate aromatic acceptor ligands and distortion patterns of their lowest energy triplet excited states. Inorg. Chem. 54, 8508.

Park, J., Joo, J., Kwon, S.G., Jang, Y., Hyeon, T., 2007. Synthesis of Monodisperse Spherical Nanocrystals Angew. Chem. Int. Ed. 46(25), 4630–4660.

Patra, N., Dehury, N., Pal, A., Behera, A., Patra, S., 2018. Preparation and mechanistic aspect of natural xanthone functionalized gold nanoparticle. Mater. Sci. Eng. C. 90, 439–445.

Patra, S., Mishra, S., 2022. Heterodimetallic iridium-rhenium system: Synthesis, computational and photocatalytic aspects. J. Photochem. Photobiol.,A. 436, 114407.

Patra, S., Yang, H., 2009. Synthesis of trimetallic Au@Pb core-shell nanoparticles and their electrocatalytic activity toward formic acid and methanol. Bull. Korean Chem. Soc. 30(7), 1485-1488.

Rahul, K., Shekhar, S., 2021. Ruthenium based antifungal compounds and their activity. Res. J. Chem. Environ. 25(7), 177-182.

Rawat, S., Singh, J., 2022a. Fabrication of iron nanoparticles by reusing an iron waste and their application as efficient adsorbents to remove crystal violet dye from water. J. Appl. Sci. Innov. Technol. 1(2), 37–46.

Rawat, S., Singh, J., 2022b. Degradation of para-nitrophenol by green synthesised iron nanoparticles: Optimization of the process parameters and study of degradation kinetics. J. Appl. Sci. Innov. Technol. 1(1), 21–26.

Rycenga, M., Wang, Z., Gordon, E., Cobley, C.M., Schwartz, A.G., Lo, C.S., Xia, Y., 2009. Probing the photothermal effect of gold-based nanocages with surface-enhanced Raman scattering (SERS). Angew. Chem. Int. Ed. 48(52), 9924–9927.

Sahoo, A., Patra, S., 2020. A magnetically separable and recyclable g-C_3N_4/Fe_3O_4/porous ruthenium nanocatalyst for the photocatalytic degradation of water-soluble aromatic amines and azo dyes. RSC Adv. 10(10), 6043–6051.

Sahoo, A., Patra, S., 2018. A Combined process for the degradation of azo-dyes and efficient removal of aromatic amines using porous silicon supported porous ruthenium nanocatalyst. ACS Appl. Nano Mater. 1(9), 5169–5178.

Schmid, G., 1992. Large clusters and colloids. Metals in the embryonic state. Chem. Rev. 92(8), 1709–1727.

Sebastián, V., Lee, S.-K., Zhou, C., Kraus, M.F., Fujimoto, J.G., Jensen, K.F., 2012. One-step continuous synthesis of biocompatible gold nanorods for optical coherence tomography. Chem. Commun. 48(53), 6654.

Segala, K., Pereira, A.S., 2012. From ruthenium complexes to novel functional nanocomposites: Development and perspectives. "New polymers for special applications."

Szewczyk, O.K., Roszczenko, P., Czarnomysy, R., Bielawska, A., Bielawski, K., 2022. An overview of the importance of transition-metal nanoparticles in cancer research. Int. J. Mol. Sci. 23(12).

Tripathy, S.K., De, U., Dehury, N., Pal, S., Kim, H.S., Patra, S., 2014. Dinuclear [{(p-cym) RuCl} 2 (μ-phpy)](PF 6) 2 and heterodinuclear [(ppy) 2 Ir (μ-phpy) Ru (p-cym) Cl](PF 6) 2 complexes: synthesis, structure and anticancer activity. Dalt. Trans. 43(39), 14546–14549.

Valente, A., Morais, T.S., Teixeira, R.G., Matos, C.P., Tomaz, A.I., Helena Garcia, M., 2021. "Ruthenium and iron

metallodrugs: New inorganic and organometallic complexes as prospective anticancer agents" in Hamilton, E.J.M. "*Synthetic Inorganic Chemistry*", Elsevier.

Venkatesan, R., Pichaimani, A., Hari, K., Balasubramanian, P.K., Kulandaivel, J., Premkumar, K., 2013. Doxorubicin conjugated gold nanorods: A sustained drug delivery carrier for improved anticancer therapy. J. Mater. Chem. B. 1(7), 1010–1018.

Vilvamani, N., Chhatwal, M., Bhowmick, I., Gupta, R.D., Awasthi, S.K., 2016. Gold nanocomposite assemblies using functionalized Ru(II)-polypyridyl complexes. RSC Adv. 6(60), 55507–55513.

Cite this article:
Kalyan, I., Sahu, K.K., Nayak, A.K., 2023. Development of Ruthenium metal functionalized gold nanoparticles. J. Appl. Sci. Innov. Technol. 2 (2), 58-67.